Numerical modelling of rock plastic yielding

Lidija Frgić, Krešimir Tor and **Antonia Jaguljnjak-Lazarević**
Faculty of Mining, Geology and Petroleum Engineering, University of Zagreb, Pierottijeva 6,
HR-10000 Zagreb, CROATIA
e-mail: lfrgic@rudar.rgn.hr; ktor@rudar.rgn.hr; ajagu@rudar.rgn.hr

SUMMARY

The concentration of stress around the opening occurs in the excavation of an opening in the rock massif. The paper discusses the changes of stress and strains in close surrounding of the elliptical opening as well as the impact of the opening on the environment. The theoretical solution is used to define dimensions of the area where the opening causes changes in the stress condition related to the primary condition within acceptable boundaries. The comparison of the results from numerical estimates is presented according to the finite elements method with results according to the theory of elasticity. Numerical estimates were performed for the cases of assuming edge conditions: forces and displacements. The assumption of the boundary condition with displacements gives better approximation of the conditions of stresses and strains.

The concentration of stress around the opening and the occurrence of the plastification zone is discussed on the case of the road tunnell excavation. The estimation is carried out according to the finite elements method using the Hoek-Brown failure criterion which is implemented into the program. The results from the stability analysis point to the area where we can expect the rock material failure, respectively the places in which the safety measures should be provided. The zones of plastification extension are graphically presented. Especially important is the comparison of the numerical modelling results with observations on the site during excavation.

Key words: *underground room, plastic yielding, finite element method.*

1. INTRODUCTION

When considering underground room planning, one of significant factors is the concentration of stress around the openings of underground rooms. Opening the whole profile of an underground room leads to a change of stress condition in close surroundings of the opening. By opening the excavation, the primary stress condition in the massif turns into the secondary condition of stress and strain depending on the rate of the progress in the exavation and supporting and on other circumstances in the area of the excavation face. The concentration of normal stresses on the opening edge takes place thereby while the shear and radial stresses disappear [1]. The impact of the opening disappears completely at some distance, so the massif outside the impact zone is in primary stress condition.

The part of the rock directly extracted cannot possibly be supported simultaneously. The stress condition and the deformation condition for such unsupported sections are estimated for the plane condition of deformations which is in accordance with the stress condition at some distance from the face itself.

The support systems' planning methods depend on local circumstances, massif properties and applied procedures of excavation and supporting. By real condition modelling, the behaviour of underground room during exavation can be foreseen. The formation of natural materials as rock and soil, in complex geologic processes is conditioned by a very wide range of physical-mechanical parameters (e.g. uniaxial compressive strength, modulus of deformation, angle of friction, cohesion and others) and spatial heterogeneity.

The stability and safety of an opening depend also on the mechanical properties of rock or soil; therefore, for the description of elastic, plastic and viscous properties of a massif it is necessary to know a great number of material characteristics. As the characteristics cannot usually be proved until certain location is found

by excavation and as they are valid only for a limited area, they are assumed on the basis of experience, whereby it is necesary to adopt possible values.

Since all the complexity of the problem cannot possibly be comprised it is necessary to apply some simplifications.

The criteria for defining safety can be based on displacements and relative deformations, stresses in the rock massif or soil, primary support and lining and the degree of plastic behaviour and bearing capacity in the sense of the ultimate state theory. The safety factors for each of the mentioned cases can be different.

2. THEORETICAL ANALYSIS OF PLANE STRAIN STATE CONDITION

The stress estimate for plane condition of deformations according to the theory of elasticity gives the first information about the occurrence near the opening. The theoretical solution is used to define dimensions of the area where the opening causes changes in the stress condition related to the primary condition within acceptable limits in the application of numerical methods: the method of finite differences, the method of finite elements or the method of boundary elements.

The underground room at certain depth can be observed as an opening in an infinite plate (Figure 1). The Poeschl solution [2] for elliptical opening will be presented here. Dimensions of the opening are given with semi-axes of the ellipses *a* nad *b*. The load *p* closes with a bigger semi-axes of ellipse *a* the angle *a*.

Fig. 1 Underground opening

The stress function F expressed by curvilinear coordinates x and h can be written as:

$$F = \frac{p \cdot c^2}{8} \left\{ \begin{array}{l} sh\,2x - cos\,2a \cdot e^{-2(x-x_0)} - \\ - 2(ch\,2x_0 + cos\,2a) \cdot x + \\ + [ch\,2(x-x_0) - 1] \cdot e^{2x_0} \cdot cos\,2(h-a) \end{array} \right\} \quad (1)$$

satisfying Maxwell's differential equation:

$$\nabla^4 F = 0 \quad (2)$$

and boundary conditions for:

$$x = \infty \quad s_y = p_h \quad s_z = p_v$$
$$x = x_0 \quad s_{xx} = t_{xh} = 0 \quad (3)$$

The stress components are the function of the stress function F:

$$s_{xx} = \frac{1}{h_2^2} F_{,hh} + \frac{1}{h_1^2 h_2} h_2{}_{,x} F_{,x} - \frac{1}{h_2^3} h_2{}_{,h} F_{,h} \quad (4)$$

$$s_{hh} = \frac{1}{h_1^2} F_{,xx} - \frac{1}{h_1^3} h_1{}_{,x} F_{,x} + \frac{1}{h_1 h_2^2} h_1{}_{,h} F_{,h} \quad (5)$$

$$t_{xh} = \frac{1}{h_1 h_2} F_{,xh} + \frac{1}{h_1^2 h_2} h_1{}_{,h} F_{,x} + \frac{1}{h_1 h_2^2} h_2{}_{,x} F_{,h} \quad (6)$$

respectively:

$$s_{xx} = \frac{2}{c^2(ch\,2x - cos\,2h)} \cdot \frac{pc^2}{2} \cdot e^{2x_0} \cdot [1 - ch\,2(x-x_0)] \cdot cos\,2(h-a) + \frac{sh\,2x}{\sqrt{ch\,2x - cos\,2h}} \cdot$$

$$\cdot \frac{4}{c^3\sqrt{2(ch\,2x - cos\,2h)^3}} \cdot \frac{c\sqrt{2}}{2} \cdot \frac{pc^2}{4} \cdot \left\{ \begin{array}{l} ch\,2x + cos\,2a \cdot e^{-2(x-x_0)} - cos\,2a - ch\,2x + \\ + sh\,2(x-x_0) \cdot e^{2x_0}\,cos\,2(h-a) \end{array} \right\} - \quad (7)$$

$$- \frac{c\sqrt{2}}{2} \cdot \frac{pc^2}{4} \cdot \frac{4}{c^3\sqrt{2(ch\,2x - cos\,2h)^3}} \cdot \frac{sin\,2x}{\sqrt{ch\,2x - cos\,2h}} \cdot e^{2x_0} \cdot [1 - ch\,2(x-x_0)] \cdot sin\,2(h-a)$$

$$s_{hh} = \frac{2}{c^2(ch\,2x - cos\,2h)} \cdot \frac{pc^2}{2} \cdot e^{2x_0} \cdot \left\{ sh\,2x + cos\,2a \cdot e^{-2(x-x_0)} + ch\,2(x-x_0) \cdot e^{2x_0}\,cos\,2(h-a) \right\} -$$

$$- \frac{1}{c^3\sqrt{2(ch\,2x - cos\,2h)^3}} \cdot \frac{c\sqrt{2}}{2} \cdot \frac{pc^2 \cdot sh\,2x}{\sqrt{ch\,2x - cos\,2h}} \left\{ \begin{array}{l} ch\,2x + cos\,2a \cdot e^{-2(x-x_0)} - ch\,2x_0 - \\ - cos\,2x + sh\,2(x-x_0) \cdot e^{2x_0}\,cos\,2(h-a) \end{array} \right\} + \quad (8)$$

$$+ \frac{4}{c^3\sqrt{2(ch\,2x - cos\,2h)^3}} \cdot \frac{c\sqrt{2}}{2} \cdot \frac{sin\,2h}{\sqrt{ch\,2x - cos\,2h}} \cdot \frac{pc^2}{4} \cdot e^{2x_0} [1 - ch\,2(x-x_0)] \cdot sin\,2(h-a)$$

$$t_{xh} = \frac{2}{c^2(ch\,2\boldsymbol{x}-cos\,2\boldsymbol{h})}\cdot\frac{pc^2}{2}\cdot e^{2\boldsymbol{x_0}}\,sin\,2(\boldsymbol{h}-\boldsymbol{a})\cdot sh\,2(\boldsymbol{x}-\boldsymbol{x_0})+ \frac{4}{c^3\sqrt{2(ch\,2\boldsymbol{x}-cos\,2\boldsymbol{h})^3}}\cdot\frac{c\sqrt{2}}{2}\cdot\frac{pc^2}{4}\cdot$$

$$\cdot\frac{sin\,2\boldsymbol{h}}{\sqrt{ch\,2\boldsymbol{x}-cos\,2\boldsymbol{h}}}\cdot\left\{ch\,2\boldsymbol{x}+cos\,2\boldsymbol{a}\cdot e^{-2(\boldsymbol{x}-\boldsymbol{x_0})}-ch\,2\boldsymbol{x_0}+cos\,2\boldsymbol{a}+sh\,2(\boldsymbol{x}-\boldsymbol{x_0})\cdot e^{2\boldsymbol{x_0}}\,cos\,2(\boldsymbol{h}-\boldsymbol{a})\right\}+ \qquad (9)$$

$$+\frac{4}{c^3\sqrt{2(ch\,2\boldsymbol{x}-cos\,2\boldsymbol{h})^3}}\cdot\frac{c\sqrt{2}}{2}\cdot\frac{pc^2}{4}\cdot\frac{sh\,2\boldsymbol{x}}{\sqrt{ch\,2\boldsymbol{x}-cos\,2\boldsymbol{h}}}\cdot e^{2\boldsymbol{x_0}}\left[1-ch\,2(\boldsymbol{x}-\boldsymbol{x_0})\right]\cdot sin\,2(\boldsymbol{h}-\boldsymbol{a})$$

where:

$$h_1^{\,2} = h_2^{\,2} = \frac{a^2 - b^2}{2}\cdot(ch\,2\boldsymbol{x} - cos\,2\boldsymbol{h}) \qquad (10)$$

Alongside the elliptical opening the circular stress is given by expression:

$$\boldsymbol{s_{hh}} = \frac{sh\,2\boldsymbol{x_0} - cos\,2\boldsymbol{a}\cdot e^{2\boldsymbol{x_0}} + cos\,2(\boldsymbol{h}-\boldsymbol{a})}{ch\,2\boldsymbol{x_0} - cos\,2\boldsymbol{h}}\cdot p \quad (11)$$

For the estimate of the secondary stress condition a program has been developed which computes the stresses in individual points on the basis of input data. The calculation is performed for the ratio of ellipse half-axis $b/a=1/2$, $2/3$ and $3/2$ and for a different ratio of the horizontal and vertical load $p_h/p_v=0$, 0.5 and 1.0.

The analytical solution according to the theory of elasticity is used to define the necessary comprising area in the analysis of stress and strain using the finite element method [3].

3. NUMERICAL ANALYSIS OF STRESS AROUND THE OPENING

More complex problems of the continuum mechanics e.g. irregular geometry of the opening cannot be solved by a mathematical formulation. It is not possible to obtain the solution in a closed form.

By numerical estimation methods we obtain approximate solutions, that is solutions of different approaches towards the solution of the problem with unlimited area [4, 5]. Using the finite element method, the most common engineering approach is the limitation or shortening of the area where the finite part is singled out from the observed infinite area in such a way that finite edges with appropriate boundary conditions are positioned far enough from the area of interest [6, 7]. In such an approach, there is a basic problem i.e. how far from the opening edge the outer boundaries should be set to get a satisfying solution [8, 9]. The boundaries are mostly set arbitrary, based on the experince or intuition [10].

Therefore the estimation is performed for different relations of semi-axes of the ellipse b/a and the load p_h/p_v. The cutting points of confocal ellipses $\boldsymbol{x}=constant$ and of confocal hyperbolas $\boldsymbol{h}=constant$ are chosen as nodal points defining the elements. The network of quadry-lateral elements is adopted. Element dimensions are increasing constantly towards the outer edge. This does not cause a slighter approximation since on the outer contour edge the stress condition approximates the homogeneous one with smaller gradients of deformations and stresses. The outer contour is assumed in the elipse form which is confocal with opening and very approximately corresponds to the circle. The symmetry of displacement and load is provided with vertically and horizontally movable supports in the axis of symmetry. The boundary conditions on the outer contour are assigned in two ways: by assigning the load - forces in the contour points (case 1) and by assigning the displacement in the contour points (case 2). For boundary conditions assumed with diplacements (case 2) it is necessary to assume in each contour point two boundary elements. The vertical and horizontal forces for the points of the outer contour are determined by the trapezoid rule:

$$P_{v\,n} = \frac{\boldsymbol{D}\,y_{n-1}}{6}\left(p_{v,n-1} + 2\,p_{v,n}\right) + \frac{\boldsymbol{D}\,y_n}{6}\left(2\,p_{v,n} + p_{v,n+1}\right) \; (12)$$

$$P_{h,n} = \frac{\boldsymbol{D}\,z_{n-1}}{6}\left(p_{h,n-1} + 2\,p_{h,n}\right) + \frac{\boldsymbol{D}\,z_n}{6}\left(2\,p_{h,n} + p_{h,n+1}\right) \; (13)$$

Displacements of contour points are obtained by integration of deformations' components:

$$v = \int \boldsymbol{e}_{yy}dy = -\frac{p_v\left(1-\boldsymbol{n}^2\right)}{E}\cdot\left(k - \frac{\boldsymbol{n}}{1-\boldsymbol{n}}\right)y \quad (14)$$

$$w = \int \boldsymbol{e}_{zz}dz = -\frac{p_v\left(1-\boldsymbol{n}^2\right)}{E}\cdot\left(1 - k\cdot\frac{\boldsymbol{n}}{1-\boldsymbol{n}}\right)z \quad (15)$$

The network of quadry-lateral elements is adopted for the elliptical opening with relation of semi-axis $b/a=1/2$. Distribution of stresses along the axes y and z for load ratio $k=0.0$ is presented in Table 1; $k=0.5$ in Table 2 and $k=1.0$ in Table 3.

Table 1 Values of stresses $\boldsymbol{s}_y$ and $\boldsymbol{s}_z$ along the axes y and z

$b/a = 1/2$ $p_v = 1.0$ and $p_h=0.0$					
y/a	$\boldsymbol{s}_z$	$\boldsymbol{s}_y$	z/a	$\boldsymbol{s}_z$	$\boldsymbol{s}_y$
1.00	5.000	0.000	0.50	0.000	-1.000
1.41	1.505	0.553	1.18	0.209	-0.047
2.00	1.170	0.266	1.80	0.549	0.056
2.83	1.072	0.129	2.69	0.762	0.045
4.00	1.033	0.063	3.91	0.877	0.027
5.66	1.016	0.031	5.59	0.938	0.014
8.00	1.007	0.015	7.95	0.968	0.007
11.31	1.003	0.007	11.28	0.984	0.003
16.00	1.001	0.003	15.98	0.992	0.001

Table 2   Values of stresses s_y and s_z along the axes y and z

b/a = 1/2			p_h/p_v = 0.5		
y/a	s_z	s_y	z/a	s_z	s_y
1.00	4.500	0.000	0.50	0.000	0.000
1.41	1.511	0.782	1.18	0.302	0.569
2.00	1.182	0.645	1.80	0.612	0.591
2.83	1.079	0.571	2.69	0.794	0.558
4.00	1.037	0.535	3.91	0.896	0.532
5.66	1.018	0.517	5.59	0.947	0.516
8.00	1.008	0.508	7.95	0.973	0.508
11.31	1.004	0.504	11.28	0.986	0.504
16.00	1.002	0.502	15.98	0.993	0.502

Table 3   Values of stresses s_y and s_z along the axes y and z

b/a = 1/2			p_h/p_v = 1.0		
y/a	s_z	s_y	z/a	s_z	s_y
1.00	4.000	0.000	0.50	0.000	1.000
1.41	1.517	1.011	1.18	0.395	1.185
2.00	1.194	1.024	1.80	0.676	1.126
2.83	1.086	1.014	2.69	0.832	1.070
4.00	1.041	1.007	3.91	0.915	1.037
5.66	1.020	1.003	5.59	0.957	1.019
8.00	1.009	1.001	7.95	0.978	1.009
11.31	1.004	1.000	11.28	0.989	1.004
16.00	1.002	1.000	15.98	0.995	1.002

The obtained values of stresses along the axis are compared with the values of the primary stresses state for the ratio of horizontal and vertical loads p_h/p_v=0.5 for the discussed opening. The differences of stress conditions for the case of opening related to primary stress state, expressed in percentages are presented in Table 4. It is obvious, that stress differences along the axis y are almost twice smaller than along the axis z.

Table 4   Differences in stresses related to primary stress along y and z axis

D(%)	10.0	5.0	2.5	0.5
y/a	2.6	3.5	5.3	10.7
z/b	4.0	5.6	7.8	19.5

Similar results are also obtained for other relations of the axis b/a=2/3 - 3/2 and load ratio p_h/p_v=0, 0.5 and 1.0. Therefore, a sixfold value of the greater semi-axis is suggested for the dimension of the comprised area. The adoption of a larger area would require a considerably larger number of nodal points and elements and a larger extension of the numerical estimation, whereby a greater accuracy in satisfying boundary conditions would not at the same time increase the accuracy of the numerical solution. This would not have any sense for the mathematical modelling of underground rooms, since greater mistakes in planning underground rooms are possible in the estimation of physical-mechanical characteristics of the massif.

For the elliptical opening with a semi-axis relation b/a=2/3, since it is approximately the ultimate case occurring in underground room construction, with p_v=1.0, stresses s_y and s_z are compared in midpoints of the elements' side along the axis y (Table 5), in midpoints of the elements side along the axis z (Table 6) and in centroids of elements along the opening (Table 7) for both ways of assuming boundary conditions: forces (Case 1) and displacements (Case 2).

Stress differences between theoretical and numerical solutions are presented in percentages of the basic vertical load p_v=1. The mean values of stress differences $D_{average}$ are presented in tables. The biggest deviations occur in the places of the greatest stress concentrations in assuming boundary conditions by forces. Assuming boundary conditions by displacements gives more accurate stresses both near the opening and on the outer contour.

Especially interesting is the comparison of the displacements of nodal points v and w of the outer contour. Considerable deviations from the theoretical solution are obtained in the case of assuming boundary conditions with forces (Case 1) in the outer contour points. The errors in displacements on the outer contour in assuming boundary conditions by forces amount to 11% theoretical value. Case 2 reproduces displacements which are assumed as boundary conditons in advance.

Table 5   Comparison of stresses s_y and s_z along the axis y in midpoints of the elements' sides

El.	Stress s_y Theory of elasticity	Case 1	D (%)	Case 2	D (%)	Stress s_z Theory of elasticity	Case 1	D (%)	Case 2	D (%)
I.	0.498	0.397	10.1	0.354	14.4	2.462	2.726	26.4	2.400	6.2
II.	0.501	0.571	7.0	0.463	3.8	1.550	1.945	39.5	1.443	10.7
III.	0.352	0.348	0.4	0.332	2.0	1.258	1.317	5.9	1.177	8.1
IV.	0.233	0.214	1.9	0.221	1.2	1.136	1.1881	4.5	1.066	7.0
V.	0.150	0.124	2.6	0.146	0.4	1.077	1.109	3.2	1.016	6.1
VI.	0.096	0.067	2.9	0.098	0.2	1.045	1.060	1.5	0.995	5.0
VII.	0.062	0.028	3.4	0.066	0.4	1.027	1.013	1.4	0.998	3.9
VIII.	0.039	0.003	3.6	0.047	0.5	1.017	0.959	5.8	0.996	2.1
		$D_{average}$	4.0	$D_{average}$	2.9		$D_{average}$	11.0	$D_{average}$	6.1

Table 6 Comparison of stresses s_y and s_z along the axis z in midpoints of the elements' sides

El.	Stress s_y Theory of elasticity	Case 1	D (%)	Case 2	D (%)	Stress s_z Theory of elasticity	Case 1	D (%)	Case 2	D (%)
I.	- 0483	- 0.598	11.5	- 0.452	3.1	- 0.023	0.035	5.8	0.036	5.9
II.	- 0.075	- 0.153	7.8	-0.088	1.3	0.171	0.221	5.0	0.208	3.7
III.	0.033	- 0.028	6.1	0.011	2.2	0.408	0.467	5.9	0.421	1.3
IV.	0.052	0.007	4.5	0.032	2.0	0.598	0.659	6.1	0.588	1.0
V.	0.045	0.016	2.9	0.024	2.1	0.733	0.801	6.8	0.710	2.3
VI.	0.034	0.024	1.0	0.009	2.5	0.826	0.897	7.1	0.793	3.3
VII.	0.023	0.042	1.9	- 0.010	3.3	0.887	0.962	7.5	0.849	3.8
VIII.	0.015	0.080	6.5	-0.034	4.7	0.927	1.006	7.9	0.887	4.0
		$D_{average}$	5.3	$D_{average}$			$D_{average}$	6.5	$D_{average}$	3.2

Table 7 Comparison of stresses s_y and s_z in centroids of elements along the opening

El.	Stress s_y Theory of elasticity	Case 1	D (%)	Case 2	D (%)	Stress s_z Theory of elasticity	Case 1	D (%)	Case 2	D (%)
I.	0.494	0.445	4.9	0.396	9.8	2.445	2.747	30.2	2.416	2.9
II.	0.354	0.324	3.0	0.292	6.2	2.243	2.459	21.6	2.167	7.6
III.	0.155	0.166	1.1	0.158	0.3	1.872	1.991	11.9	1.762	11.0
IV.	- 0.024	0.004	2.8	0.022	4.6	1.399	1.438	3.9	1.285	11.4
V.	- 0.161	- 0.142	1.9	- 0.098	6.3	0.922	0.907	1.5	0.823	9.9
VI.	- 0.261	- 0.270	0.9	- 0.199	6.2	0.515	0.487	2.8	0.452	6.3
VII.	- 0.348	- 0.405	5.7	- 0.301	4.7	0.221	0.214	0.7	0.205	1.6
VIII.	- 0.429	- 0.531	10.2	- 0.399	3.0	0.053	0.074	2.1	0.075	2.2
IX.	- 0.483	- 0.607	12.4	- 0.460	2.3	- 0.015	0.020	3.5	0.024	3.9
		$D_{average}$	4.8	$D_{average}$	4.8		$D_{average}$	8.7	$D_{average}$	6.3

4. FAILURE CRITERION

In order to analyse the underground room stability in the excavation it is necessary to define the failure criterion i.e. the stress condition where deformations become unlimited. For cohesive and non-cohesive soils Mohr-Coulomb's failure criterion is suitable (Figure 2), which is expressed by intensities of the main stresses:

$$\frac{s_1 + s_3}{2} - \frac{s_1 - s_3}{2} \cdot \sin j = c \cdot \cos j \qquad (16)$$

where:
  s_1 and s_3 - principal stresses $[kN/m^2]$
  c - cohesion $[kN/m^2]$
  j - friction angle [°].

The Hoek-Brown failure criterion is formed in rock mechanics for the rock massif [11, 12]:

$$s_1 = s_3 + \sqrt{m s_c s_3 + s s_c^2} \qquad (17)$$

where:
  s_1 - critical compressive stress $[kN/m^2]$
  s_3 - minimum compressive stress $[kN/m^2]$
  m - Hoek-Brown coefficient
  s - Hoek-Brown coefficient
  s_c - uniaxial compressive rock strength $[kN/m^2]$.
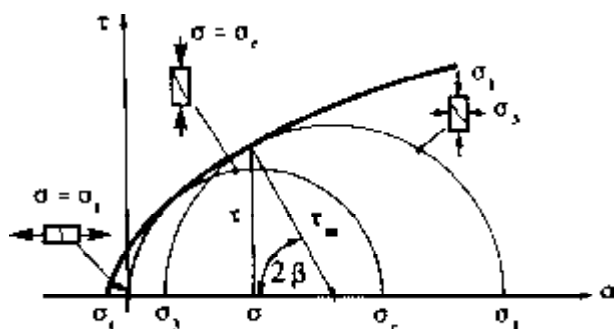
Fig. 2 Mohr-Coulomb failure criterion
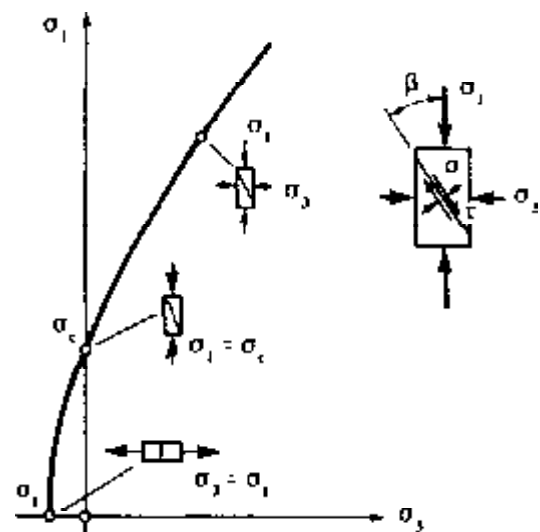
Fig. 3 Hoek-Brown failure criterion

The application of this criterion enables perceiving of the area in which tensile failure or sliding occurs. The relation between the critical stress and the estimation stress represents an apparent safety coefficient. To prove the existence or non-existence of the plastic deformation it is necessary to compare the degree of the effective stress of the observed point with the equivalent stress of relaxation. The occurrence and the way of development of plastification zone around the opening was performed by the finite element method. For this purpose, the Hoek-Brown material failure criterion was implemented in the programme of finite elements with elastic model of material behaviour, since it suits best the rock behaviour in the case of tunnel excavation.

As an example we take estimates of the conditions of stress and strain in the excavation of the road tunnel by opening the whole profile [13]. The choice of the needed number, the forms and dimensions of elements are based on preliminary comparisons. The networks of finite elements were generated and the serendipity elements were used. Regarding the vertical symmetry axis, only one half of the profile was observed, whereby the assmption was simplified. The size of the observed area was adopted as sixfold value of the lager dimension of the opening. The stress condition on the outer contour, which is a circle, can be considered approximately homogeneous. Towards the outer contour a constant step of dimension elements' increase is adopted due to smaller and smaller gradients of deformation and stress. By vertically movable displaceable supports in the symmetry axis, the displacement symmetry was also realized. As the load, the upper-bed weight of the massif was taken, i.e. the massif pressure corresponding to primary stress states:

$$p_v = r \cdot g \cdot z \qquad (18)$$

$$p_h = k \cdot p_v \qquad (19)$$

The action of gravity loading of elements is modelled by the concept of initial stresses in Gauss' points without subsidence occurrence, which is the only one acceptable in the analysis of rock and soil mechanics. Graphic representations of the computation results are given for the rock of the third category of tunnel excavation. An overburden height of *150 m* is assumed. The following values of the rock massif are adopted in the estimate:

Uniaxial strength	s_c = 20 - 50 MN/m^2
Hoek-Brown coefficient	m = 1.0 - 3.5
Hoek-Brown coefficient	s = 0.01 - 0.1
Density	r = 2.5 t/m^3
Young's modulus	E = 10,000 MN/m^2
Poisson's ratio	n = 0.25
Ratio of horizontal and vertical pressure	$k = p_h/p_v$ = 0.75

Figure 4 illustrates the plastic zones for the case *m=3.5, s=0.1* and *s_c=25 MN/m^2*.
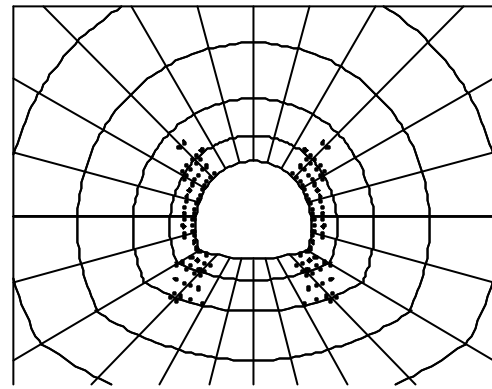
Fig. 4 Plastic zones for the case m=3.5; s=0.1 and s_c=25 MN/m^2

The Gauss' points plastified according to Hoek-Brown's criterion of failure were determined with the "PLAST" programme. The estimation results filed by a special Fortran programme are converted into the script record convenient for drawing in AUTOCAD. The Gauss' points with plastification occurrence are marked with a circle.

The influence of separate input parameters is analyzed, and that is why the changes of Hoek-Brown's coefficient *m* are presented on Figure 5 and the change of coefficient *s* in Figure 6. By reason of symmetry the plastification zones are marked only for one half of the tunnels' cross-section.
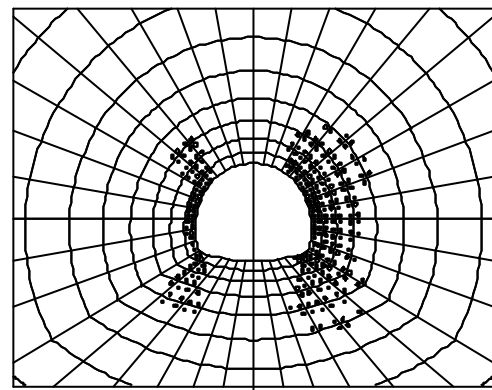
Fig. 5 Plastic zones obtained by variation of failure coefficient m for the cases s=0.1 and s_c=25 MN/m^2
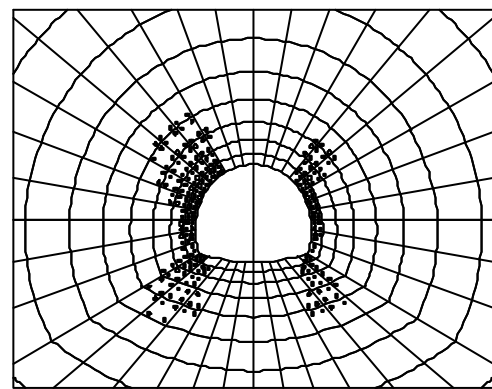
Fig. 6 Plastic zones obtained by variation of failure coefficient s for the cases m=3.5 and s_c=25 MN/m^2

Plastification zones for different values of uniaxial strength s_c with rock massif coefficient $m=3$ and $s=0.1$ are presented in Figure 7.
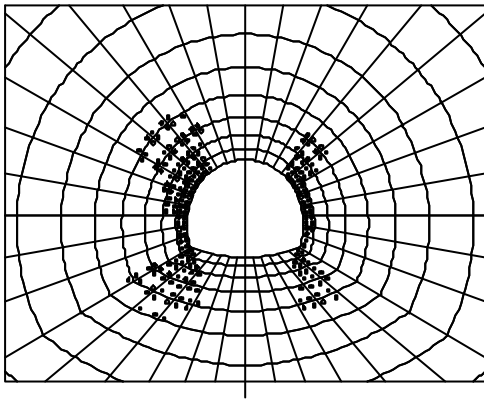
Fig. 7 Plastic zones obtained by uniaxial strength variation for the case m=3 and s=0.1

The massif in the flowing state is presented by a boundary line, which is in the final presentation in ACAD rounded with option "fit line". Contour lines in Figure 8 for the case $m=3.5$ and $s=0.1$ are presented with different values of a uniaxial strength s_c. Each line represents in fact a certain safety coefficient according to Hoeck-Brown failure criterion. The size of the plastic zones does not depend only on Hoek-Brown's coefficients and uniaxial strength but it also depends on the ratio of horizontal and vertical initial pressures.

Although these results are more qualitative than quantitative they point to the form of plastic zones which also has a practical meaning. In supporting with anchors, the anchorages should not be located in plastic zones because thereby the bearing capacity of the anchors would be questionable. With supporting we also strengthen the rock wherewith we improve the physical and mechanical properties of the rock and in this way prevent further plastic deformations.

5. CONCLUSION

The conditions of stress and strains around the opening are analyzed according to the finite element method. According to the results from the theory of elasticity the six-fold value of the greater semi-axis is suggested as an optimal value of the comprised area. The comparison of the results obtained from numerical estimations with the theoretical solution indicates that, assuming the boundary condition with displacements (Case 2), gives a better approximation of stresses and strains than assuming the boundary conditions with forces (Case 1).

For the estimation of the states of stresses and strains around the tunnel profile opening the Hoek-Brown failure criterion was adopted. By implementation of the Hoek-Brown failure criterion into the program of finite elements for the elastic

continuum, the stability analysis of the opening stability in the tunnel excavation was improved. The opening stability was estimated by the variation of physical-mechanical massif characteristics. The places of the occurrence and the way in which the zones of plastification extend are graphically presented. For determining the mechanical characteristics of the rock/soil possible deviations from the average values have to be considered. The estimate assumptions have to be checked by in-situ measurements on a tunnel pilot section and used to improve the computation model.
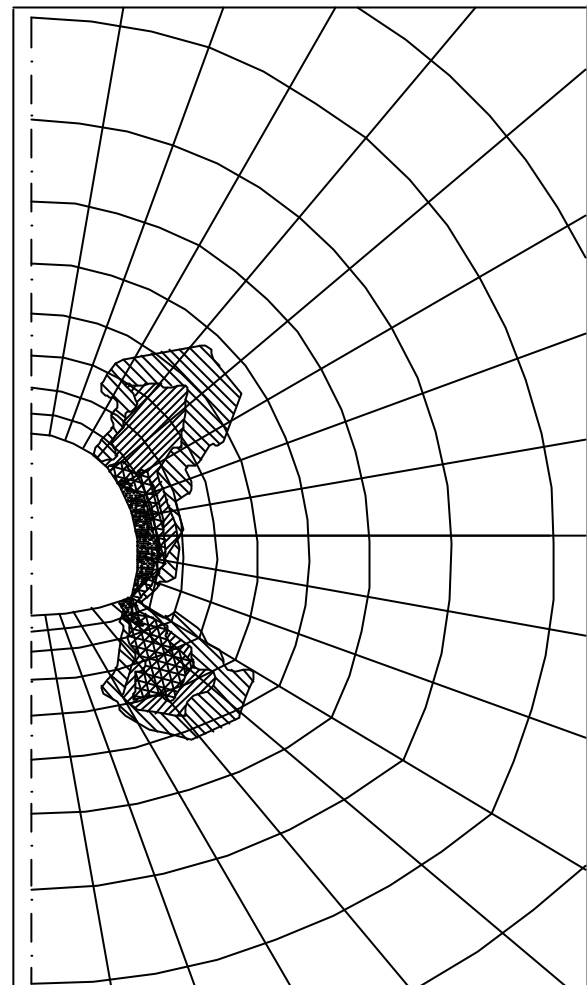
Fig. 8 Plastic zones represented by contour lines for the case m=3.5, s=0.1 and various values of uniaxial strength s_c

6. REFERENCES

[1]   G.N. Savin, *Stress Concentration Around Holes*, Pergamon Press, 1961.

[2]   T. Poeschl, Ueber eine partikulaere Loesung des biharmonischen Problems fuer den Aussenraum der Ellipse, Zeitschr. f. Math., 1921.

[3] L. Frgiæ, M. Magerle and K. Tor, Influence of boundary conditions on stress and strain results near underground rooms, Proc. 2nd Congress of Croatian Society of Mechanics, Eds. P. Maroviæ, J. Soriæ and N. Vrankoviæ, pp. 157-164, 1997.

[4] G. Gudehus, *Finite Elements in Geomechanics*, John Wiley & Sons, London, 1977.

[5] O.C. Zienkiewicz, *The Finite Element Method*, McGraw-Hill Book Co., 1977.

[6] C.S. Desai and J.T. Christian, *Numerical Methods in Geotechnical Engineering*, McGraw-Hill, New York, 1977.

[7] H. Mang and C. Kropik, Computational Mechanics of the Excavation of Tunnels, NATM, IACS, Wien, 1995.

[8] D.J. Naylor, G.N. Pande, B. Simpson and R. Tabb, *Finite Elements in Geotechnical Engineering*, Pineridge Press Ltd., Swansea, 1991.

[9] O.C. Zienkiewicz and Y.K. Cheung, *The Finite Element Method in Structural and Continuum Mechanics*, McGraw-Hill Book Co., 1967.

[10] M. Hudec, Statics of underground room support, Rock mechanics - Foundations - Underground works, Croatian Society of Civil Engineers, pp. 905-998, Zagreb, 1983.

[11] E. Hoek, *Rock Engineering, course notes*, Author/Internet, Vancouver, 1999.

[12] E. Hoek and E.T. Brown, *Underground Excavations in Rock*, Institution of Mining and Metallurgy, p. 527, London, 1980.

[13] L. Frgiæ, K. Tor and A. Jaguljnjak-Lazareviæ, Stress analysis in homogeneous medium during tunnel excavation, Proc. 3rd Congress of Croatian Society of Mechanics, Cavtat-Dubrovnik, Ed. P. Maroviæ, pp. 201-208, 2000.

NUMERIÈKO MODELIRANJE PLASTIÈNOG POPUŠTANJA STIJENSKOG MASIVA

SAŽETAK

U radu su prikazane promjene naprezanja i deformacija u neposrednoj okolini otvora podzemne prostorije. Iskopom podzemne prostorije u stijenskom masivu dolazi do koncentracije naprezanja uz otvor. Teorijsko rješenje za eliptièni otvor korišteno je za određivanje velièine podruèja u kojem postojanje otvora izaziva promjene u stanju naprezanja u odnosu na primarno stanje unutar prihvatljivih granica. U tu je svrhu napravljen program kojim se proraèunava sekundarno stanje naprezanja. Dana je usporedba rezultata numerièih proraèuna po metodi konaènih elemenata s rezultatima po teoriji elastiènosti. Numerièki proraèuni provedeni uz zadavanje rubnih uvjeta: silama (sluèaj 1) i pomacima (sluèaj 2) te je konstatirano da zadavanje rubnih uvjeta pomacima daje bolju aproksimaciju stanja naprezanja i deformacija. Koncentracija naprezanja uz otvor i pojava zona plastifikacija obrađena je na primjeru iskopa cestovnog tunela. Proraèun je proveden po metodi konaènih elemenata programom u koji je implementiran Hoek-Brownov kriterij loma koji dobro opisuju ponašanje stijena u sluèaju iskopa. Rezultati analize stabilnosti ukazuju na podruèja u kojima možemo oèekivati slom stijenskog materijala odnosno mjesta na kojima treba poduzeti mjere osiguranja. Usporedba rezultata numerièkih modeliranja i samih opažanja na terenu prilikom iskopa od posebnog je znaèaja.

Ključne rijeèi*: podzemna prostorija, plastièno popuštanje, metoda konaènih elemenata.*